Local Heating Transforms Amorphous Calcium Carbonate to Single Crystals with Defined Morphologies

Shuheng Zhang, Ouassef Nahi, Xuefeng He, Li Chen, Zabeada Aslam, Nik Kapur, Yi-Yeoun

Kim and Fiona C. Meldrum

T (°C)	Growth rate (μm s ⁻¹)
140	0.006
150	0.011
160	0.027

Table S1. Rate of growth of calcite in ACC films precipitated from solutions comprising [Ca²⁺] = 10 mM, [Mg²⁺] = 4 mM and [PAA] = 4 μ g mL⁻¹ as measured at different temperatures.

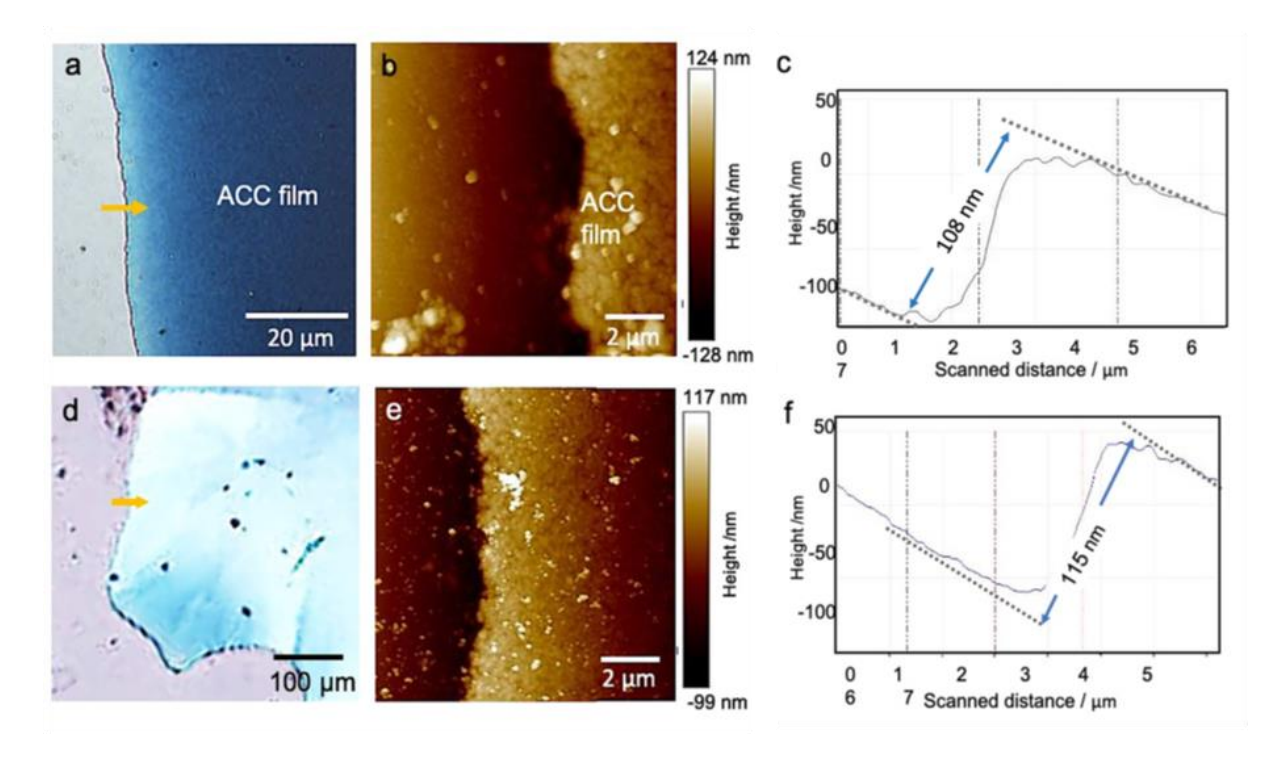


Figure S1. Characterization of the thicknesses of ACC and Mg-calcite films produced at $[Ca^{2+}]$ = $[Mg^{2+}]$ = 10 mM and [PAA] = 4 μ g mL⁻¹, where films were scratched prior to AFM analysis. Mg-calcite films were prepared by crystallizing ACC precursor films at 150 °C. (a) ACC film characterized by Polarised Optical Microscopy (POM) and (b) AFM. (c) A corresponding height profile along the direction of the yellow arrow in (a). (d) Calcite films characterized by POM, (e) characterized by AFM and (f) a corresponding height profile along the direction of the black arrow in (d).

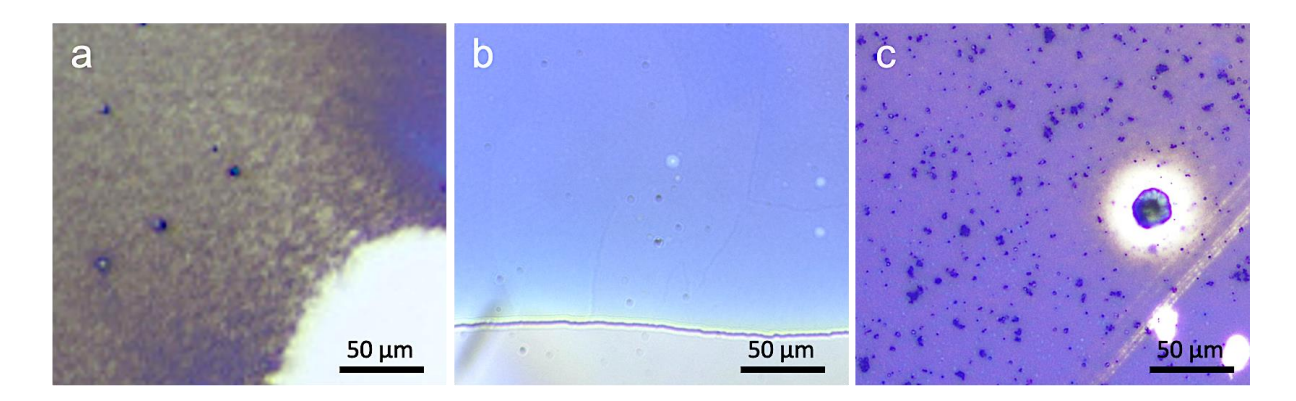


Figure S2. Optical images of ACC films deposited at (a) 10 min, (b) 30 min and (c) 40 min under the reaction conditions of $[Ca^{2+}] = [Mg^{2+}] = 10$ mM, $[PAA] = 4 \mu g mL^{-1}$.

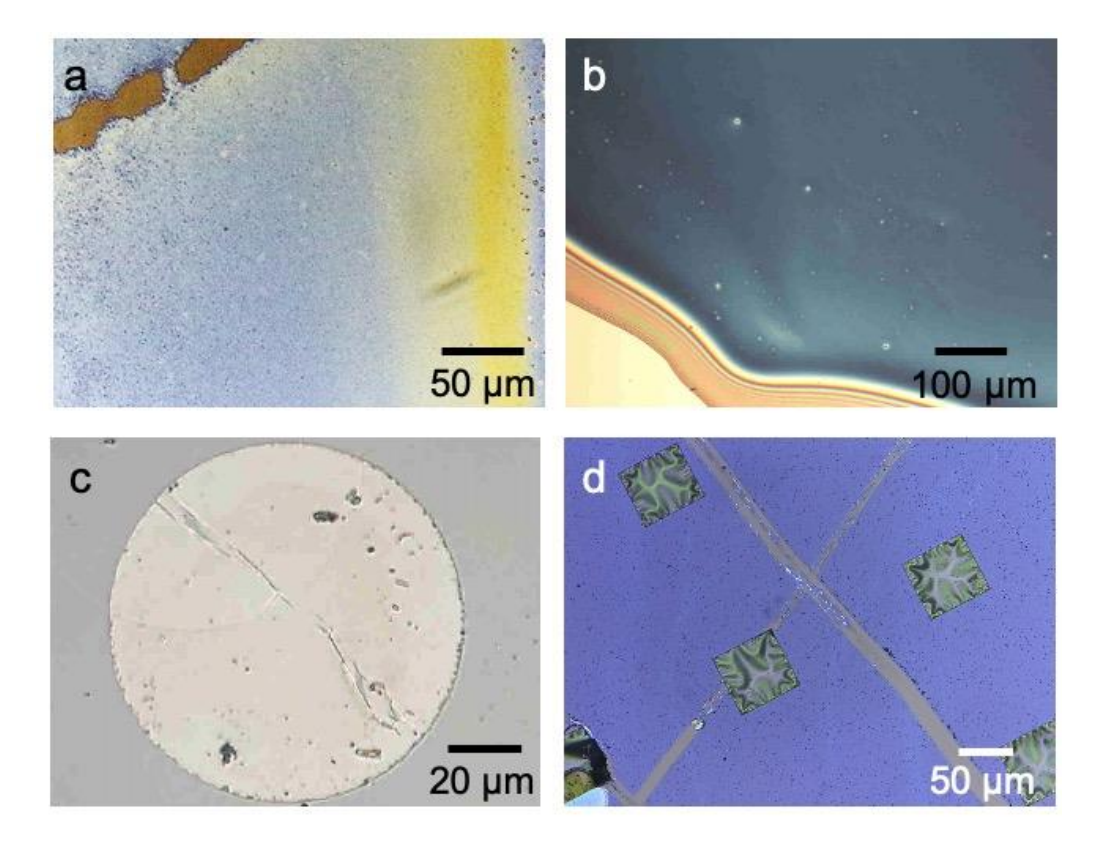


Figure S3. ACC thin films produced at $[Ca^{2+}] = [Mg^{2+}] = 10$ mM and $[PAA] = 4 \mu g mL^{-1}$ deposited on (a) poly(methyl methacrylate) (PMMA) coated glass, (b) poly(vinyl alcohol) (PVA) coated silicon wafer, (c) PDMS and (d) SiN TEM window grid. The ACC films were intentionally scratched to show the difference between substrate and films.

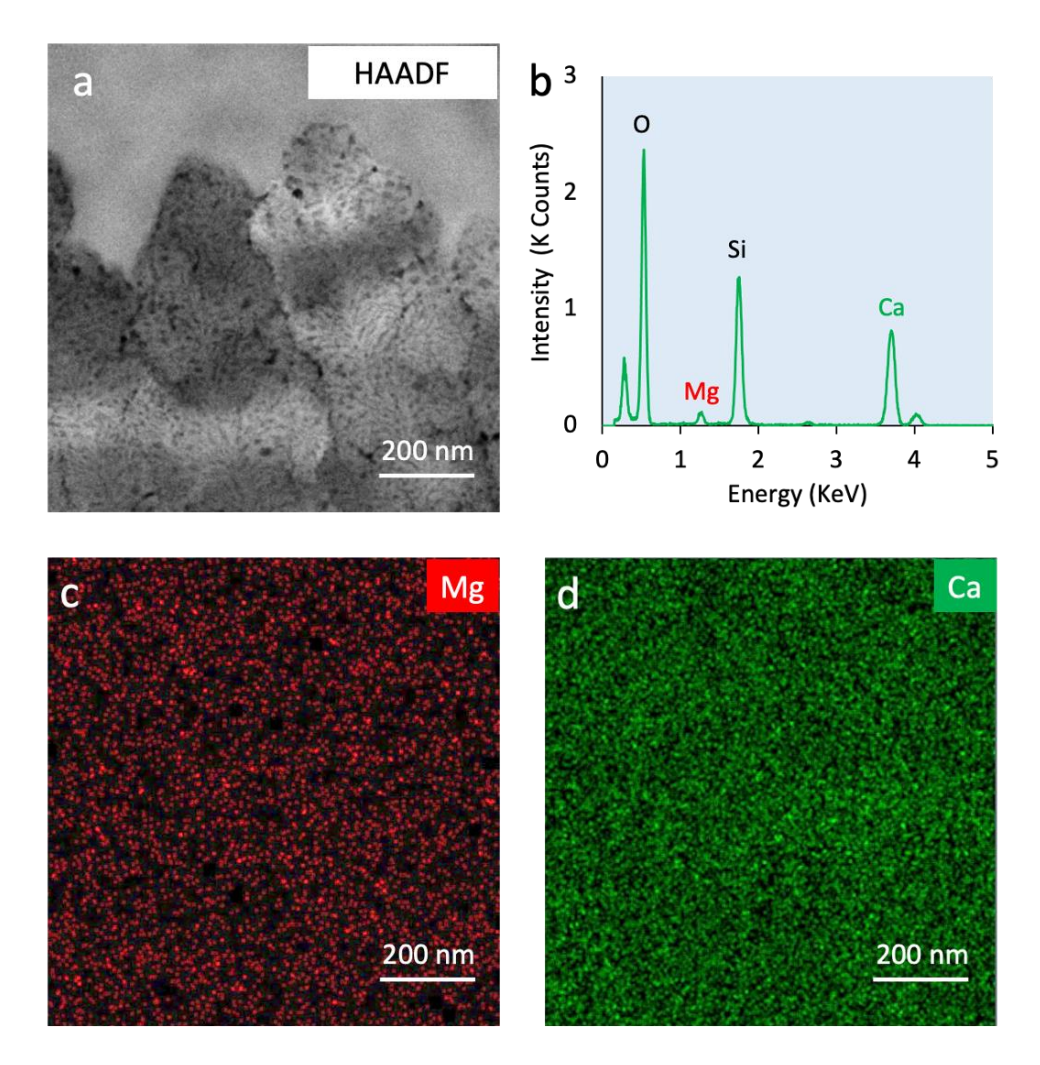


Figure S4. Elemental analysis at the ACC/ calcite interface for films produced at $[Ca^{2+}] = [Mg^{2+}] = 10 \text{ mM}$ and $[PAA] = 4 \mu g \text{ mL}^{-1}$. (a) STEM-HAADF image of Mg and Ca of a partially crystallized ACC film showing the ACC/ calcite boundary. (b) The corresponding EDX spectrum. (c and d) HAADF-EDX maps of Mg and Ca respectively taken over the same sample, showing that Ca and Mg are uniformly distributed across the ACC/ calcite interface.

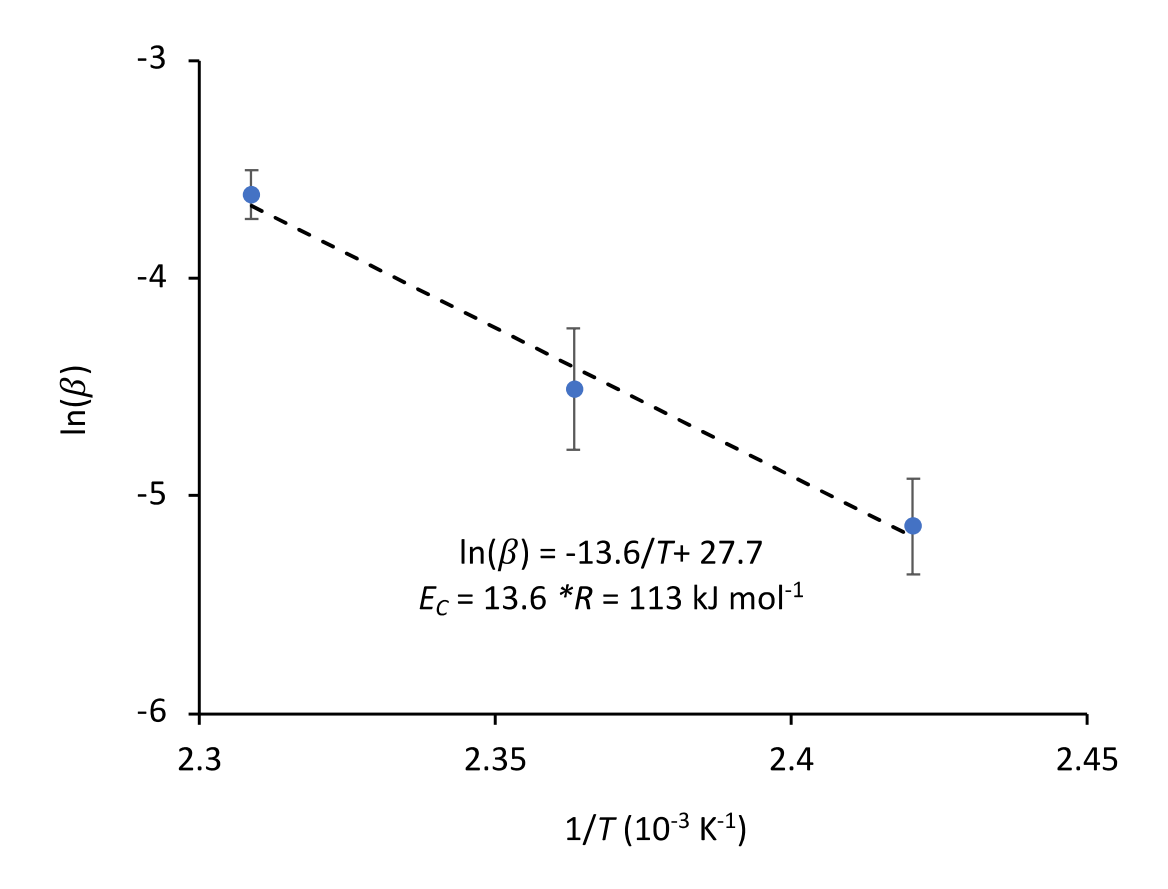


Figure S5. Graph showing the dependence of the growth rate of calcite in an ACC film (β) (μ m sec⁻¹) produced under conditions [Ca²⁺] = 10 mM, [Mg²⁺] = 4 mM, [PAA] = 4 μ g mL⁻¹ as a function of temperature. A linear relationship is seen between ln β and T⁻¹.

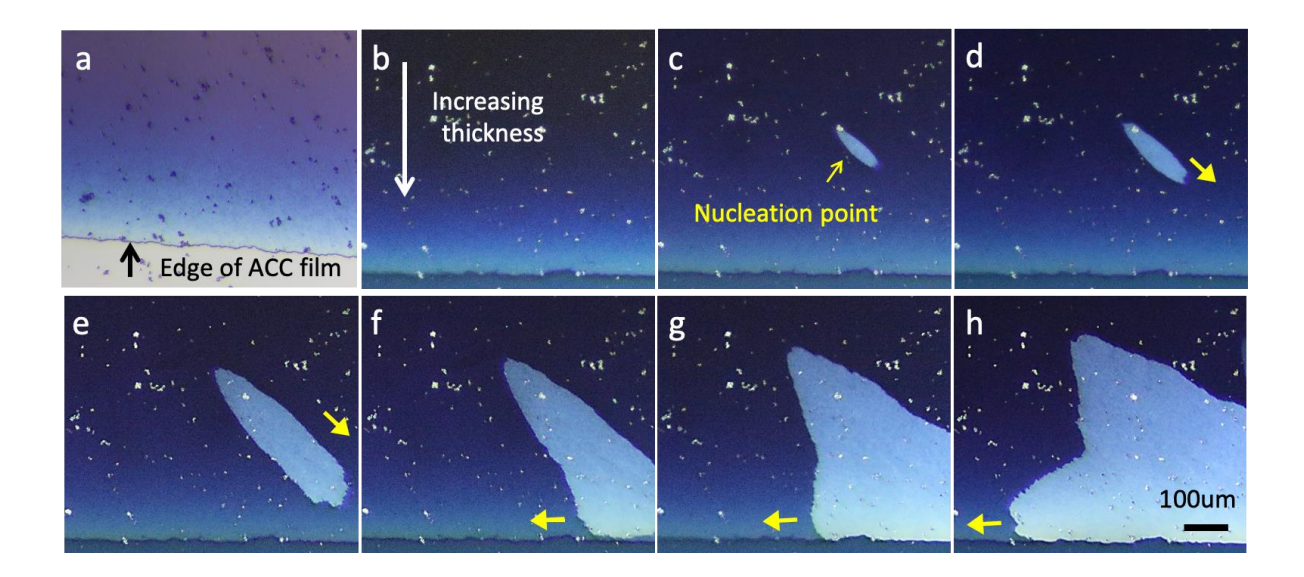


Figure S6. Thickness-dependent transformation of ACC films prepared at $[Ca^{2+}] = 10$ mM, $[Mg^{2+}] = 10$ mM and $[PAA] = 4 \mu g ml^{-1}$. The initial ACC film was imaged by (a) optical and (b) polarized optical microscopy. The gradient of colour indicates a gradient of increasing thickness from centre to edge. (c-h) POM time sequences showing the controlled process of nucleation and growth, where a single nucleation point was triggered by localized heating (c), and crystal growth was carried on by uniform heating at the second step (120°C). The preferential growth direction is indicated by the yellow arrows in (d-h).

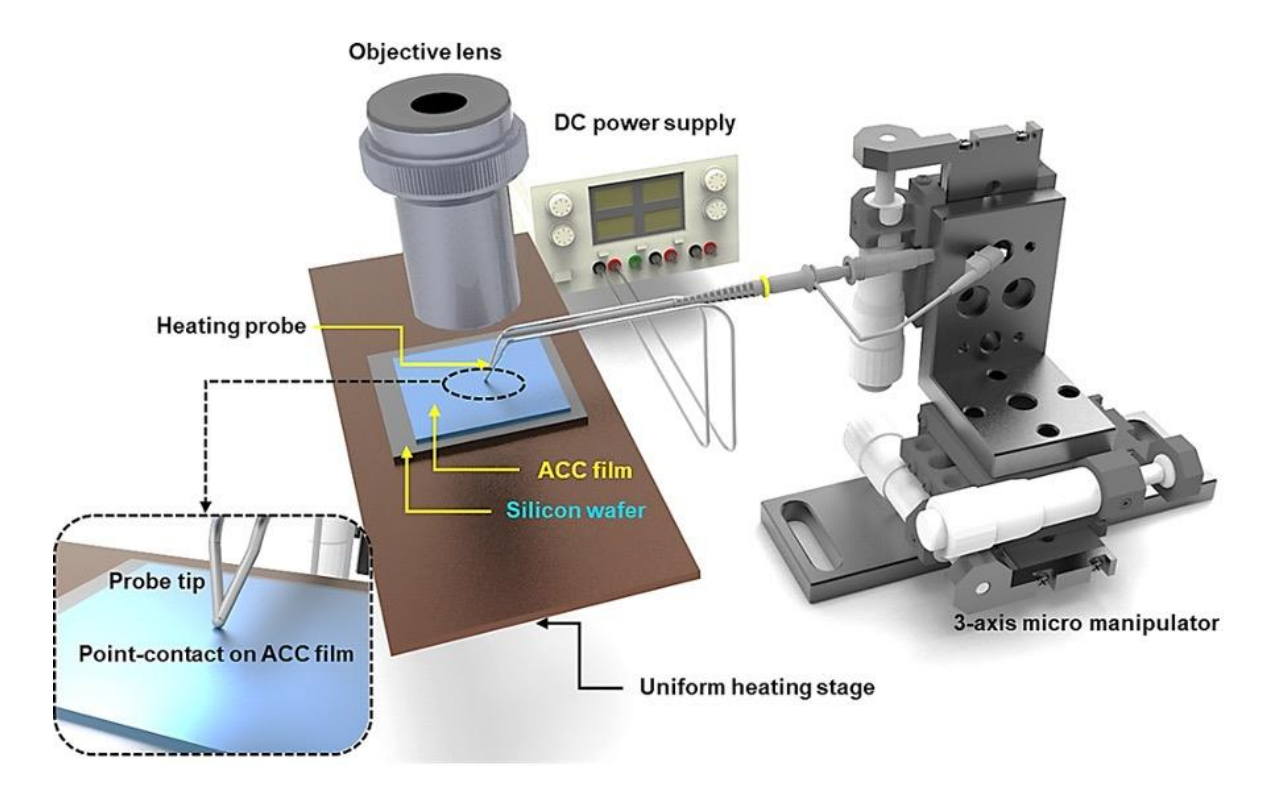


Figure S7. Schematic diagram of the experimental set-up for the controlled two-step method. Nucleation can be triggered with localized high temperature (180°C) using a joule-heated silver probe. The displacement of the silver probe is controlled by an xyz micromanipulator and the sample is positioned on a uniformly-heated stage to sustain crystal growth. POM monitors the formation and growth of the nascent crystals in real time.

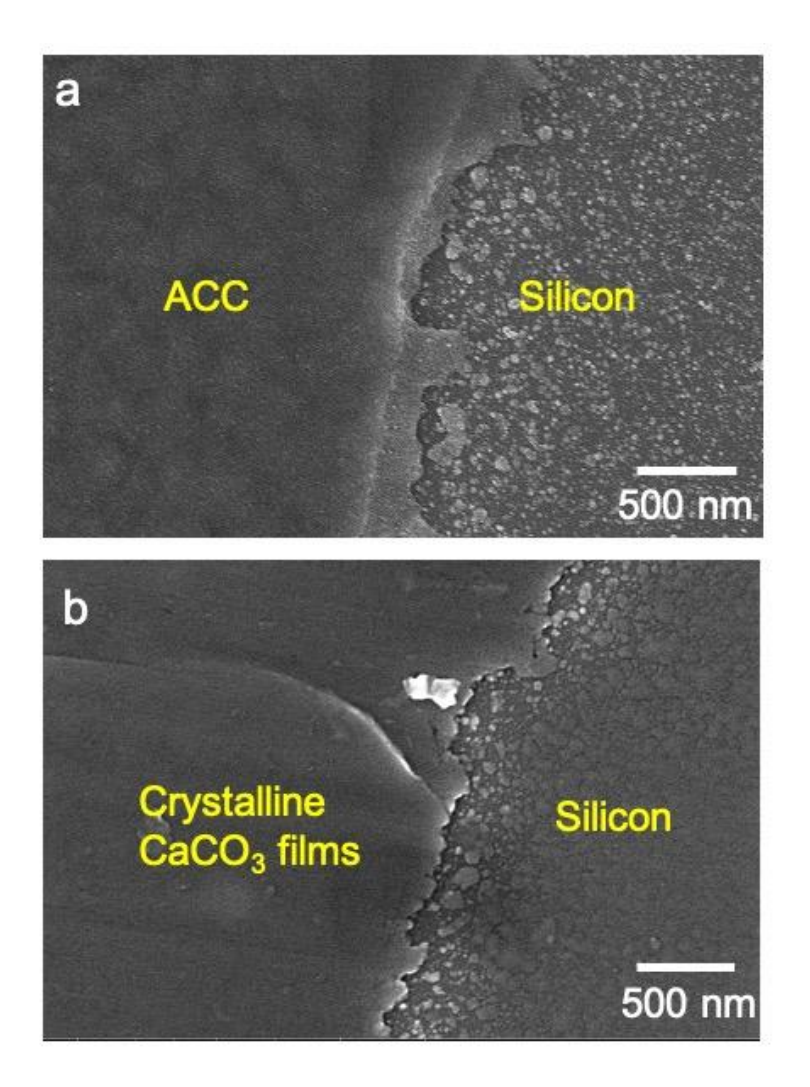


Figure S8. SEM images of ACC films produced under conditions $[Ca^{2+}] = [Mg^{2+}] = 10 \text{ mM}$ and $[PAA] = 4 \mu g \text{ mL}^{-1}$ (a) before and (b) after crystallization at 150 °C.

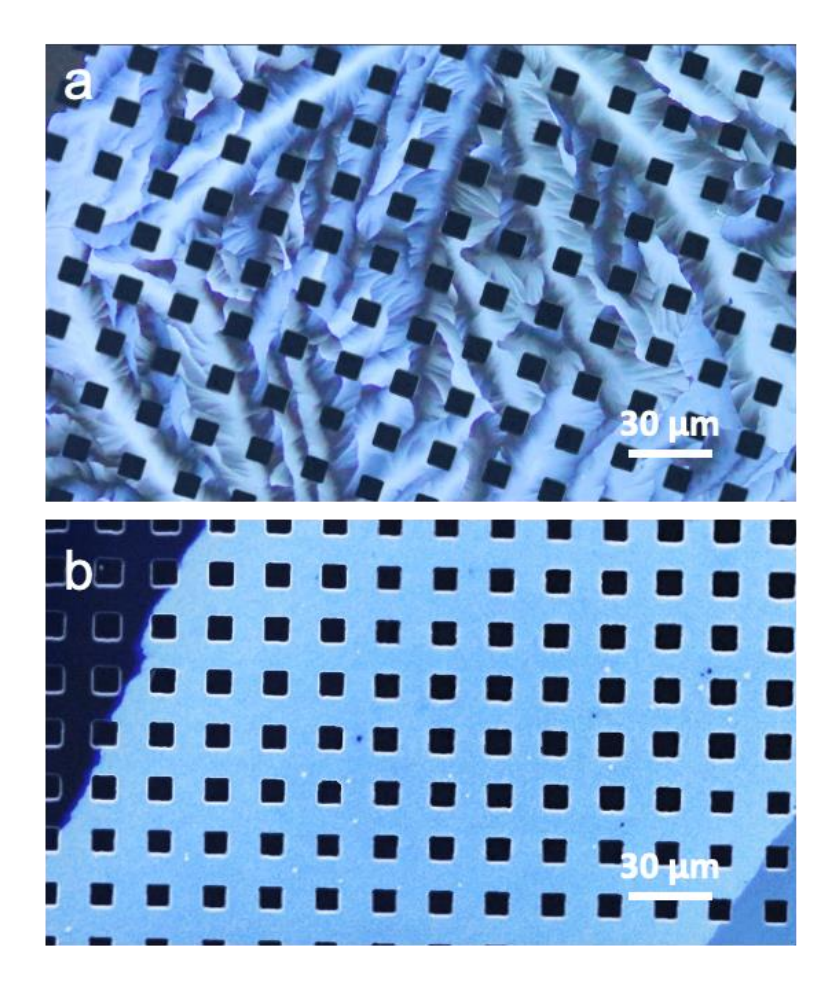


Figure S9. Calcite films formed within an array of square microposts that are 10 μ m in size and set 10 μ m apart from solution conditions [Ca²⁺] = 10 mM, [Mg²⁺] = 4 mM and [PAA] = 4 μ g mL⁻¹. (a) Calcite films with spherulitic structures were formed on crystallization at room temperature, while (b) a large, 300 μ m single crystal domain of calcite is shown that was formed using the 2-step heating method.

Movie S1. Crystallization of ACC films prepared from solutions comprising $[Ca^{2+}] = [Mg^{2+}]$ = 10 mM and $[PAA] = 4 \mu g mL^{-1}$ at $T_{ON} = 150 \, ^{\circ}C$.

Movie S2. Triggering nucleation at a single site using a local heating probe at 180 °C. The ACC film was prepared from solutions comprising $[Ca^{2+}] = [Mg^{2+}] = 10$ mM and [PAA] = 4 μg mL⁻¹.

Movie S3. Transformation of ACC films sustained with uniform heating below T_{ON} . The ACC films were prepared from solutions comprising $[Ca^{2+}] = [Mg^{2+}] = 10$ mM and [PAA] = 4 μg mL⁻¹, and incubated at 120 °C ($< T_{ON}$).

Movie S4. Crystallization of ACC films that were deposited on a silicon substrate patterned with pillars. The ACC films were prepared from solutions comprising $[Ca^{2+}] = [Mg^{2+}] = 10$ mM and $[PAA] = 4 \mu g \text{ mL}^{-1}$, and crystallized at $T_{ON} = 150 \, ^{\circ}\text{C}$.

Movie S5. Crystallization of an array of ACC discs that were prepared from solutions comprising $[Ca^{2+}] = 10$ mM, $[Mg^{2+}] = 4$ mM and [PAA] = 4 μg mL⁻¹, and crystallized at $T_{ON} = 200$ °C.